

Molecular modeling of the binding mode of chiral metal complexes Δ - and Λ -[Co(phen)₂dppz]³⁺ with B-DNA

YANG Pin (杨 频) & HAN Daxiong (韩大雄)

Institute of Molecular Science, Shanxi University, Taiyuan 030006, China

Correspondence should be addressed to Yang Pin (email: yangpin@mail.sxu.edu.cn)

Received June 20, 2000

Abstract Molecular modeling methods have been applied to the structural characterization of the interaction between chiral metal complexes [Co(phen)₂dppz]³⁺ (where phen = 1, 10-phenanthroline, dppz = dipyrido[3,2-a: 2', 3'-c]phenazine) and the oligonucleotide (B-DNA fragment). The natures of two kinds of the binding modes, which are currently intense controversy, have been explored. Barton proposed that there is enantio-selective DNA binding by the octahedral complexes and intercalative access by these complexes from the major groove; but Norden suggested that both enantiomers bind extremely strongly to DNA from the minor groove without any noticeable enantio-selectivity. Our results support and extend structural models based upon Norden's studies, and conflict with Barton's model.

Keywords: molecular modeling, MM2 forcefield, docking, B-DNA, metal enantiomers.

For the intercalative mode of the metal complexes Δ , Λ -[Ru(phen)₂dppz]²⁺ bound to DNA, it is clear from the experimental data^[1] that the planes of the chelate ligands of Δ , Λ -[Ru(phen)₂dppz]²⁺ are nearly parallel to the nucleobase plane (perpendicular to the polynucleotide helix axis). The above mode is classical intercalation and accepted by most of scientists. But there still have been divergences about intercalative orientations and enantio-selectivity. Among all sorts of viewpoints, Barton's and Norden's are the most representative ones. Barton suggested that

intercalation occurs from the major groove with two orientations of the dppz ligands in the intercalation pocket^[2], i.e. "head-on" and "side-on" fashions as in fig. 1, and DNA binding exhibits noticeable enantio-selectivity (due to steric interference, Δ -isomers bind more tightly by intercalation to right-handed duplexes than Λ -isomers do). On the contrary, Norden has proposed that the enantiomers bind to DNA from the minor groove without any noticeable enantio-selectivity^[3-5].

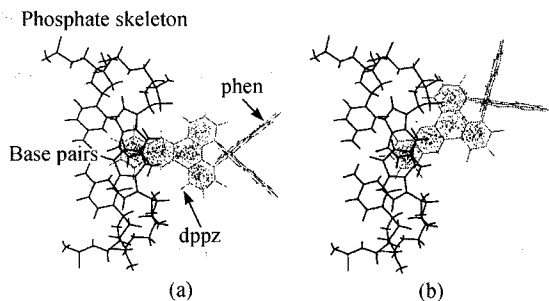


Fig. 1. Two kinds of intercalative fashions of the chiral complexes in the minor groove. (a) Picture for the "head-on" fashion, both phenazines are well protected; (b) picture for the "side-on" fashion, these axes may form an acute angle, maximizing stacking with the base pair, in which one side of the ligand is more exposed to solvent than the other, which is similar in the major groove.

To date, most of studies known are about the metal Ru complexes—DNA interactions. There is currently only a little information concerning the intercalative geometries of DNA and mixed-ligand Cobalt (III) complexes. To our knowledge, only Arounaguir^[6] and our research group^[7] carried out studies by several kinds of experimental methods. These experimental results show that a manner consists of binding by classical intercalation and enantio-selectivity to DNA. Such studies are also needed to serve as complementary studies on those kinds of systems, but have some drawbacks: (i) Without the chiral metal complexes Δ , Λ -[Cu(phen)₂dppz]³⁺ separated or the pure enantiomers synthesized, such earlier studies were unable to thoroughly explore the DNA enantio-selectivity; (ii) these work only indicated that Δ , Λ -[Co(phen)₂dppz]³⁺ could be considered as a classical DNA intercalator, but no detailed three-dimensional structure (interactive orientations and sites) has yet been solved for a chiral metal complex bound to a DNA fragment. On the basis of the above two aspects, we have explored the intercalative geometries between Δ , Λ -[Co(phen)₂dppz]³⁺ and DNA{d(GTCGAC)₂, d(AGTACT)₂ and d(GTCGACGTCG)₂} by molecular modeling methods, and further discussed whose viewpoint is more reasonable by comparing Barton's with Norden's.

1 Modeling methods

First, we built the complexes Δ , Λ -[Co(phen)₂dppz]³⁺ and the B-DNA fragments of different chain lengths [d(GTCGAC)₂ (selected by Barton), d(AGTACT)₂, and d(GTCGACGTCG)₂]. Then we carried out a complete conformational analysis for each enantiomer using MM2 force field from CS Chem3D Package. The B-DNA fragments were also minimized using MM2. Next step, the simulation of interactive orientations was carried out with the most stable conformer for each enantiomer using the docking methodology in a PC. The best relative position of each enantiomer in relation to the B-DNA double helix was found by monitoring the system energy. In other words, while manually changing the relative position of the enantiomer, the value of system energy was calculated by the minimization of the interactive system consisting of enantiomer and B-DNA fragment. Conjugate gradient to an energy gradient of 20.92 kJ · mol⁻¹ · nm⁻¹ was obtained. The process is necessary to allow the optimization of the manually model-built enantiomers orientation to seek the minimum energy of the system^[8]. After favorable intercalative orientation was obtained, through changing the depth of intercalation, we further sought the best site. In this stage, the conjugate gradient optimizer was used until an energy gradient of less than 2.092 kJ · mol⁻¹ · nm⁻¹ was obtained. All the simulation was carried out in the gaseous state.

It must be pointed out^[9] that in the docking methodology, the total intermolecular energy between two molecules is computed by non-bonded terms of the force field equation. This equation for the MM2 force field is shown below:

$$E_{\text{inter}} = \sum \sum \left(A_{ij} / r_{ij}^{12} - B_{ij} / r_{ij}^6 + q_i q_j / \epsilon r_{ij} \right),$$

where the first two terms are Lennard-Jones (6-12) potential and the last one is the Coulomb

potential. We employed a non distance-dependent dielectric, ϵ (1.5).

2 Results and discussion

It has been established that the complexes Δ , Λ -[Co(phen)₂dppz]³⁺ bound from the minor and major groove of B-DNA fragments and that the dppz ligand was inserted into a base pair (such as A-T or C-G) and double base pairs (such as GT/CA or CG/GC) of B-DNA with different intercalative depths (the intercalative depth was defined as the distance from a fixed position to another (r). In AT region, r is referred to the distance between the N of adenosine (A) NH₂ and the Co of the complexes. In CG region, r is referred to the distance between the N of cytosine (C) NH₂ and the Co of the complexes), and then explored the interactive conformation between the complexes and B-DNA was explored. We carried out the docking based upon fig. 1.

2.1 Major groove orientation

The energy minimization results of binding from the major groove are listed in table 1. When binding sites were located in the base pair T₂A₂ or A₅T₅, regardless of intercalative depth, the system energy changes a little because of terminal effects. In other binding sites when the head

Table 1 The energy minimization results of binding from the major groove

Region	Fashion	Λ -[Co(phen) ₂ dppz] ³⁺				Δ -[Co(phen) ₂ dppz] ³⁺			
		r	E (head-on)	r	E (side-on)	r	E (head-on)	r	E (side-on)
T ₂ -A ₂ region		10.2	525.01	12.0	459.49	11.1	447.31	12.1	471.70
		8.2	518.40	10.4	496.43	9.5	499.74	10.5	491.95
		6.8	511.62	8.2	426.77	7.3	518.31	8.4	499.28
C ₃ -G ₃ region		11.0	468.19	6.3	601.78	10.8	517.31	6.6	517.60
		9.0	580.03	5.4	4 312.03	8.9	532.92	5.2	5 978.52
		6.9	2 908.30	4.8	8 190.18	7.2	636.01	–	–
		–	–	–	–	4.7	4 489.01	–	–
G ₄ -C ₄ region		8.4	543.63	7.4	397.23	8.4	559.32	7.4	473.21
		7.7	3 137.50	5.7	388.11	8.0	597.81	5.8	455.60
		7.9	4 302.41	4.9	2 748.64	7.9	4 370.19	4.7	467.73
		–	–	–	–	–	–	1.6	2 604.54
A ₅ -T ₅ region		10.3	510.36	9.4	673.79	9.9	495.22	9.3	681.87
		7.9	550.99	7.5	493.84	7.8	574.80	7.8	646.18
		6.7	506.05	6.5	547.94	6.6	530.32	7.3	599.90
T ₂ A ₂ /C ₃ G ₃ region		11.3	487.98	11.7	444.08	11.1	2 754.03	11.8	438.61
		9.5	2 901.60	10.0	449.82	–	–	10.2	474.97
		–	–	8.4	457.14	–	–	8.4	531.03
C ₃ G ₃ /G ₄ C ₄ region		10.0	481.33	5.9	509.53	10.2	502.00	5.7	571.12
		7.5	658.65	4.9	472.46	8.1	543.13	4.8	649.48
		6.3	4 152.70	3.8	8 685.15	6.9	556.72	3.9	3 222.85
G ₄ C ₄ /A ₅ T ₅ region		8.9	474.42	7.6	441.16	8.8	466.43	8.0	486.81
		7.1	379.53	6.0	561.70	7.2	420.91	6.3	470.11
		6.0	440.83	5.1	3 017.88	5.9	501.16	5.7	3 082.94

Bold presents the steric energy that extremely increases; energy unit: kJ • mol⁻¹; r unit: 10⁻¹ nm; convergence criterion: 20.92 kJ • mol⁻¹ • nm⁻¹.

part of the dppz ligand of each isomer was intercalated into the base stack with “head-on” or “side-on” fashion, the steric interference was observed for van der Waals clashes (the system energy increases notably, see the bold in table 1). The main explanation of why the complexes are unable to intercalate more deeply is the steric interference of the two phenanthroline “propeller blades” with a groove. In total, the data indicate that the intercalative depth is limited only to the head of the dppz ligand and has no correlation with the intercalative regions or chiral discrimination.

2.2 Minor groove orientation

In table 2, it could be observed that while the dppz ring head, body, and even the tail intercalate the base stacks, in all the cases it does not produce steric interference. The short axis diameter (0.892 1 nm) of the complexes is smaller than the width of the major groove (2.985 7 nm) and that of the minor groove (1.585 nm), so in theory the intercalative depths should be the same regardless of the involvement of the major or minor groove. The modeling results show a noticeable difference. In the major groove, steric interference occurs when the dppz head is intercalated; on the contrary, in the minor groove, steric interference does not occur at any depth

Table 2 The energy minimization results of binding from the minor groove

Fashion Region	Δ -[Co(phen) ₂ dppz] ³⁺				Δ -[Co(phen) ₂ dppz] ³⁺			
	<i>r</i>	<i>E</i> (head-on)	<i>r</i>	<i>E</i> (side-on)	<i>r</i>	<i>E</i> (head-on)	<i>r</i>	<i>E</i> (side-on)
T ₂ -A ₂ region	13.4	493.08	13.2	487.10	13.3	478.02	13.3	458.11
	11.5	487.56	11.9	487.48	11.7	488.52	11.9	493.92
	10.7	468.86	10.2	522.21	10.4	518.98	11.1	770.19
C ₃ -G ₃ region	14.8	505.72	14.1	510.49	14.9	486.52	14.1	506.85
	13.0	677.89	13.1	655.26	12.9	733.71	13.4	575.63
	11.4	614.34	10.8	630.74	12.1	616.64	10.6	594.38
G ₄ -C ₄ region	14.6	499.70	13.8	589.32	14.6	485.64	14.4	563.88
	13.1	590.91	12.5	604.04	12.9	662.95	13.0	642.12
	11.5	741.11	9.3	677.52	12.0	672.79	10.9	562.20
A ₅ -T ₅ region	14.0	496.60	13.6	476.77	14.0	496.77	13.2	506.60
	12.3	514.88	12.6	521.66	12.3	494.26	12.0	538.44
	10.5	423.34	10.6	506.85	10.5	455.93	10.6	517.73
T ₂ A ₂ /C ₃ G ₃ region	14.1	510.53	–	–	14.1	498.73	–	–
	12.2	527.39	–	–	12.3	509.49	–	–
	10.2	475.34	9.1	456.22	10.3	498.02	9.3	479.99
	8.5	485.89	–	–	8.5	575.09	–	–
	7.3	516.98	–	–	7.9	577.98	–	–
	7.0	808.14	–	–	6.3	573.79	–	–
C ₃ G ₃ /G ₄ C ₄ region	14.5	505.05	–	–	14.5	525.09	–	–
	13.1	553.84	–	–	13.0	566.72	–	–
	11.9	552.50	11.2	549.61	10.3	612.83	11.3	598.06
	8.8	798.06	–	–	9.9	596.55	–	–
	8.7	691.99	–	–	8.7	665.51	–	–
G ₄ C ₄ /A ₅ T ₅ region	9.2	778.52	–	–	9.1	926.04	–	–
	13.8	465.97	–	–	13.7	496.77	–	–
	12.0	440.07	–	–	11.9	488.52	–	–
	10.3	407.06	10.6	548.77	10.3	408.94	10.8	400.12
	8.8	438.27	–	–	9.4	422.25	–	–
	8.7	441.50	–	–	8.7	479.40	–	–
7.8	636.80	–	–	7.6	476.60	–	–	

Energy unit: kJ · mol⁻¹; *r* unit: 10⁻¹ nm; convergence criterion: 20.92 kJ · mol⁻¹ · nm⁻¹.

selected. There are several explanations which may be seen in the following figures. (i) As fig. 2, the major groove is rich in nucleobases in comparison with the minor groove. (ii) As fig. 3, the extending orientation of the nucleobases faces the major groove. (iii) As fig. 4, the intercalative orientation of the dppz head matches the helical direction of the phosphate skeleton.

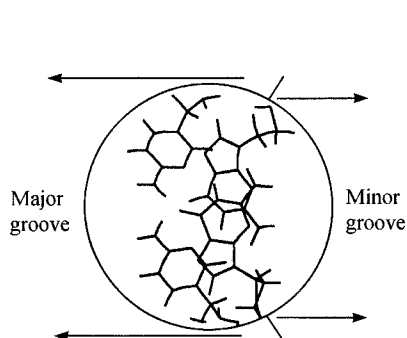


Fig. 2. Schematic representation of residues skeleton in the minor and major grooves. $>180^\circ$ is major groove, and $<180^\circ$ is minor groove.

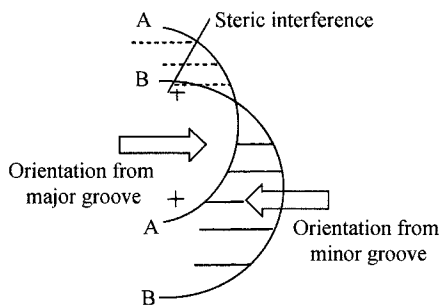


Fig. 4. Schematic representation of the correlation between the steric interference and intercalative orientation. In minor groove, the intercalative orientation is consistent with the helical direction of phosphate skeleton, so it is not easy to produce van der Waals clash; in major groove, as the phosphate skeleton forms a cone curve, it is very easy for the gigantic tail of the complexes to clash with the curve wall and produce steric interference to obstruct the dppz ligand to further intercalate.

intercalate the $T_3A_3-A_4T_4$ region of DNA $d(AGTACT)_2$. The convergence criterion was $20.92 \text{ kJ} \cdot \text{mol}^{-1} \cdot \text{nm}^{-1}$. The process of energy minimization is shown in table 3.

It can be observed that the interaction energy appears to be quite sensitive to the depth of stacking between the dppz ligand and DNA base pairs. In B-DNA $d(GTCGAC)_2$, the minimum value of the energy occurred while the dppz ligand moiety intercalated the base stacks ($364.89 \text{ kJ} \cdot \text{mol}^{-1}$ for Δ -isomer, $371.79 \text{ kJ} \cdot \text{mol}^{-1}$ for Λ -isomer). In B-DNA $d(AGTACT)_2$, it occurred while the dppz ligand moiety-tail intercalated the base stacks ($578.86 \text{ kJ} \cdot \text{mol}^{-1}$ for Δ -isomer,

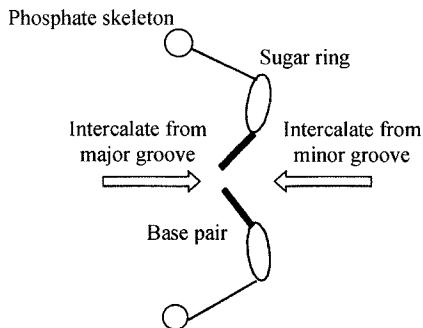


Fig. 3. Schematic representation of the orientation relationship. In the minor groove, the intercalative direction of the dppz ligand is consistent with the extending orientation of base pairs and sugar rings.

2.3 Optimum intercalative depth and enantio-selectivity

Barton suggested that the complexes intercalate the base stack in at least two fashions: "head-on" and "side-on". Here, we sought the optimum fashion through energy calculation. The result omits other interactive forces (such as electrostatic force, solvent effect). We should first select "head-on" fashion. On the basis of the above results, we made the metal complexes insert into the $C_3G_3-G_4C_4$ region (slight terminal effect) of B-DNA $d(GTCGAC)_2$ via a "head-on" fashion from the minor groove, and then explored the optimum intercalative depth and enantio-selectivity through energy calculations. Simultaneously, we made the complexes

550.24 kJ · mol⁻¹ Λ -isomer). So we suggest that for the complexes the optimal intercalative length is located in the dppz ligand moiety-tail, which was supported by Chen and Turro^[10], who made experimental studies of the interaction between Ru complexes and B-DNA. In addition, our analysis shows that both enantiomers bind extremely strongly B-DNA without any noticeable enantio-selectivity. The same optimum intercalative depth and the same obstacle position for both enantiomers can confirm this (see the energy changes in table 3).

Table 3 The energy results of the optimal sites

C ₃ G ₃ -G ₄ C ₄ region of d(GTCGAC) ₂				T ₃ A ₃ -A ₄ T ₄ region of d(AGTACT) ₂			
Λ -isomer		Δ -isomer		Λ -isomer		Δ -isomer	
<i>r</i>	<i>E</i> (head-on)	<i>r</i>	<i>E</i> (head-on)	<i>r</i>	<i>E</i> (head-on)	<i>r</i>	<i>E</i> (head-on)
16.4	434.05	16.7	431.24	14.5	689.52	14.7	694.46
14.7	428.36	14.7	433.55	12.6	655.93	12.9	655.55
13.7	403.76	13.8	409.70	10.1	586.89	10.5	599.73
11.0	371.79	10.4	364.89	8.8	592.91	9.1	611.24
9.2	441.41	11.4	403.00	7.7	550.24	8.9	578.86
10.6	437.02	10.9	407.48	7.9	573.46	8.8	635.01
8.2	3 964.80	9.1	3051.85	4.4	10 735.3	3.7	4 440.48

Bold presents the energy value of the optimum site; energy unit: kJ · mol⁻¹; *r* unit: 10⁻¹ nm.

2.4 Terminal effect

Through extending the hexanucleotide d(GTCGAC)₂ to the decanucleotide d(GTCGAC-GTCG)₂, we investigated possible changes in the optimum site and enantio-selectivity in the presence of the terminal effect. The results are shown in table 4.

Table 4 The energy minimization of the complexes binding with the C₃G₃-G₄C₄ region of B-DNA d(GTCGACGTCG)₂

Orientation of the minor groove		Orientation of the major groove	
Λ -isomer	Δ -isomer	Λ -isomer	Δ -isomer
591.50	583.68	478.57	461.07
532.37	565.19	3 121.96	2 932.38
507.60	539.18	—	—
505.78	504.20	—	—
534.05	536.97	—	—
4 810.39	3 493.87	—	—

Bold presents the energy value of the optimum site; energy unit: kJ · mol⁻¹; convergence criterion: 20.92 kJ · mol⁻¹ · nm⁻¹.

For B-DNA, the nucleobase number of a helical period is 10, so the decanucleotide already forms a whole circuit. We used it as a target molecule in order to reduce the terminal effect. The same results as for the hexanucleotide were obtained: the dppz ligand moiety-tail stacks the base pairs in the minor groove without noticeable enantio-selectivity. Therefore, the results show that the terminal effect does not change the optimum conformation of the complexes binding with the B-DNA fragment, and further confirm the results of the hexanucleotide.

2.5 Heat of formation

Molecular mechanics can be used to calculate the heat of formation (interaction energy). To do so requires the energy to form the bonds in the molecule to be added to the steric energy. The

steric energy of a given structure may vary considerably from one force field to another, but the heat of formation should be much closer. Without the breaking and formation of a bond in our modeling processes, these bond energies are not considered, and the heat of formation is simply equal to the difference between the steric energy of the two isolated species and the steric energy of the intermolecular complex. On the basis of the steric energy previously obtained (table 3), we undertook the following calculations, as table 5.

Table 5 The results of heat of formation

(kJ · mol⁻¹)

Region	Energy		Isolated species		Binding system	Heat of formation
	d(GTCGAC) ₂	d(AGTACT) ₂	Δ-isomer	Λ-isomer		
CG region	371.12	–	64.39	–	371.79	–63.72
	371.12	–	–	64.35	364.89	–70.58
AT region	–	652.58	64.39	–	550.24	–166.73
	–	652.58	–	64.35	578.86	–138.07

From table 5, we obtain three results: (i) The heat of formation has a negative value, illustrating that the binding process reduced the energy of the whole system, and that the classical intercalative mode is feasible; (ii) there is slight difference between Δ-isomer and Λ-isomer for the heat of formation. In the CG region, the steric energy of the Δ-isomer decreases more than that of Λ-isomer. In the AT region, the steric energy of Λ-isomer significantly decreases. All cases demonstrate that neither the Δ-isomer nor the Λ-isomer has priority to binding with the B-DNA fragment; (iii) the heat of formation of T₃A₃-A₄T₄ region is nearly twice as much as that of the C₃G₃-G₄C₄ region. The data indicate that the complexes may have some sequence selectivities in their binding with the hexanucleotide. Here, the complexes bind at the AT/TA site of the B-DNA fragment. We suggest that the sequence selectivity may be due to favorable minor groove dimensions in these sequences.

Finally, we obtain the optimum binding conformation between the metal complexes Δ, Λ-[Co(phen)₂dppz]³⁺ and B-DNA fragment through molecular modeling, as shown in figs. 5 and 6. The lateral view (fig. 5) clearly indicates that with the plane of the intercalative ring system approximately parallelling to the plane of the base, the dppz ring system spans the stacked base pairs (intercalation) and extends into the major groove, and that though the complexes insertion makes the base pairs fully separate, the basic B-type conformation of the oligonucleotide is maintained. In fig. 6, the binding geometries of the enantiomers in B-DNA, with the complexes tail(phen ring) rotating slightly clockwise around the complex 2-fold axis(before optimization the angle shown in fig. 6 is 31°, after optimization the roll angle for Λ-isomer is 1° and that for Δ-isomer is 5°), are not very different from those in B-DNA with similar, minor variations between the enantiomers. From the tail-wing size, the other two phenanthroline ligands of the metal complexes are proposed to be located in the minor groove of B-DNA fragment.



Fig. 5. The lateral view of the optimum binding conformation.

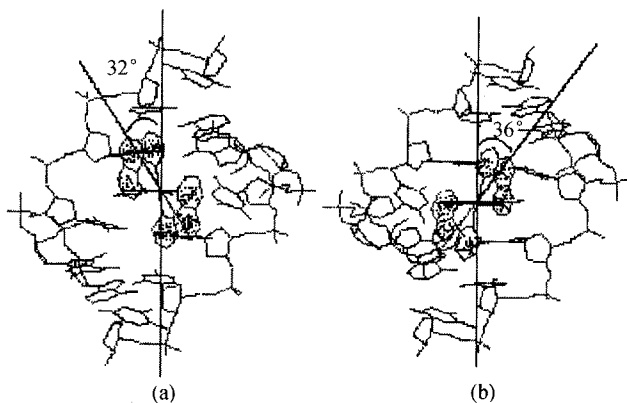


Fig. 6. The optimum conformation of $[\text{Co}(\text{phen})_2\text{dppz}]^{3+}$ binding with B-DNA from the minor groove. (a) About Δ , (b) about Λ .

3 Conclusions

Our study represents a rare situation in which it is possible to characterize the structural details of the interactions of both the Δ -isomer and the Λ -isomer with the DNA oligonucleotides through the application of molecular modeling. Four important conclusions are drawn:

(i) The complexes binding B-DNA via classical intercalation and the intercalative probability from the minor groove are significantly greater than those from the major groove.

(ii) Both the Δ and the Λ complexes bind by intercalation of this dppz planar moiety-tail between the DNA base pairs.

(iii) Both enantiomers bind B-DNA without any noticeable enantio-selectivity.

(iv) The possible AT sequence selectivity is observed in binding models between the Δ , Λ - $[\text{Co}(\text{phen})_2\text{dppz}]^{3+}$ and B-DNA fragments $\{\text{d}(\text{GTCGAC})_2$ and $\text{d}(\text{AGTACT})_2\}$.

In all, we agree with Norden's viewpoint, whereas Barton's major groove binding model and the enantio-selectivity are not supported by our molecular modeling results.

References

- Pyle, A. M., Rehmann, J. P., Barton, J. K. et al., Mixed-ligand complexes of ruthenium (II): Factors governing binding to DNA, *J. Am. Chem. Soc.*, 1989, 111: 3051.
- Cynthia, M. D., Barton, J. K., Structural studies of Λ - and Δ - $[\text{Ru}(\text{phen})_2\text{dppz}]^{2+}$ bound to $\text{d}(\text{GTCGAC})_2$: Characterization of enantioselective intercalation, *Inorg. Chem.*, 1997, 36: 33.
- Catharina, H., Lincon, P., Norden, B., DNA binding of Λ - and Δ - $[\text{Ru}(\text{phen})_2\text{dppz}]^{2+}$, *J. Am. Chem. Soc.*, 1993, 115: 3448.
- Eimer, T., Per, L., Bengt, N., Photophysical evidence that Λ - and Δ - $[\text{Ru}(\text{phen})_2\text{dppz}]^{2+}$ intercalate DNA from the minor groove, *J. Am. Chem. Soc.*, 1997, 119: 239.
- Per, L., Bengt, N., DNA binding geometries of ruthenium (II) complexes with 1, 10-phenanthroline and 2, 2'-bipyridine ligands studied with linear dichroism spectroscopy, borderline cases of intercalation, *J. Phys. Chem. B*, 1998, 102: 9583.
- Arounaguir, S., Maiva, B. G., Dipyrrophenazine complexes of cobalt (III) and nickel (II): DNA-binding and photocleavage, *Inorganic Chemistry*, 1996, 35: 4267.
- Jin, L., Yang, P., Synthesis and DNA binding studies of Co(III) mixed-ligand complex, *Polyhedron*, 1997, 16(19): 3395.
- Santos-Filho, O. A., Figueroa-Villar, J. D., Molecular modeling of the interaction of trypanocide guanyl hydrazones with B-DNA, *Bioorganic & Medicinal Chemistry Letters*, 1997, 7(13): 1797.
- Burkert, U., Allinger, N. L., *Molecular Mechanics*, Washington DC: American Chemical Society, 1982.
- Chen, W., Claudia, T., Nicholas, J. et al., Resonance Raman investigation of $\text{Ru}(\text{phen})_2(\text{dppz})^{2+}$ and related complexes in water and in the presence of DNA, *J. Phys. Chem. B*, 1997, 101: 6995.